AJNR

Congenital nasal masses: CT and MR imaging features in 16 cases.

A J Barkovich, P Vandermarck, M S Edwards and P H Cogen

AJNR Am J Neuroradiol 1991, 12 (1) 105-116
http://www.ajnr.org/content/12/1/105

Congenital Nasal Masses: CT and MR Imaging Features in 16 Cases

A. James Barkovich[1,2]
Pierre Vandermarck[1]
Michael S. B. Edwards[2]
Philip H. Cogen[2]

The imaging studies of 16 children with pathologically proved nasal encephaloceles (eight), nasal dermal sinuses/nasal dermoids (seven), and nasal cerebral heterotopias, more commonly known as nasal gliomas (one), were retrospectively reviewed and compared with normal control subjects to define the normal anatomy and analyze deformities caused by these lesions. Nasal encephaloceles were always identified as complex masses of mixed soft tissue and CSF intensity that were contiguous with intracranial structures. The nasal glioma appeared as a mixed-intensity mass that, on the basis of the CT scan, appeared to be continuous with intracranial structures. Nasal dermal sinuses could only be identified as they coursed through the skin and subcutaneous soft tissue. They could not be identified when intraosseous. Moreover, on CT and, particularly, on MR, a number of potential diagnostic pitfalls were encountered. The most important of these was the normal fat deposition that occurs within bone during normal maturation and during aeration of the frontal sinuses and nasal bones. These fatty changes can easily be mistaken for fatty tumors if they are not recognized as normal anatomic changes. Interestingly, the classic plain film findings for congenital nasal masses were present only in the encephaloceles and nasal glioma; dermoids and dermal sinuses showed none of the classic plain film findings. In the six patients who had both CT and MR, the masses were easily identified and characterized by each imaging method.

Congenital nasal masses are well characterized by both CT and MR. It is important to understand the normal changes in the anatomy of the nasofrontal region in the pediatric age group to avoid false-positive diagnoses in this region.

***AJNR* 12:105–116, January/February 1991; *AJR* 156: March 1991**

The congenital midline nasal masses are rare anomalies; their rate of occurrence is approximately one in every 20,000–40,000 live births [1, 2]. The most common of these masses are dermoid/epidermoid tumors (almost always associated with dermal sinus tracts), nasal cerebral heterotopias (nasal gliomas), and nasal encephaloceles [1–6]. Less common masses include simple inclusion cysts, hemangiomas, and aberrant ethmoidal sinuses [2].

When pediatric patients present with a midline nasal mass or a nasal dimple, an imaging study is usually obtained to better characterize and delineate the disease and to plan for appropriate therapeutic intervention. We have found, however, that the complex anatomy and often subtle findings make interpretation of these images difficult. In this report, we define the normal embryology and anatomy of the frontonasal region in infants and children, and then present the CT and MR features of 16 patients who presented with congenital midline nasal masses.

Materials and Methods

The imaging studies of 16 children with pathologically proved nasal encephaloceles (eight), nasal dermoids/dermal sinuses (seven), and nasal gliomas (one) were retrospectively reviewed

Received February 22, 1990; revision requested June 14, 1990; revision received July 15, 1990; accepted July 24, 1990.

[1] Department of Radiology, Neuroradiology Section, University of California, San Francisco, 505 Parnassus Ave., San Francisco, CA 94143-0628. Address reprint requests to A. J. Barkovich.

[2] Department of Neurological Surgery, Division of Pediatric Neurosurgery, University of California, San Francisco, CA 94143.

0195-6108/91/1201-0105

TABLE 1: Patient Data

Patient No.	Age	Sex	Imaging Method	Diagnosis	Presentation	FC Size (mm)	Crista		Mass				IOD (mm)	Associated Anomalies
							Size (mm)	Bifid	Location	Size (mm)	MR	CT		
1	3 mo	F	CT	DS dermoid	Nasal mass	5	4	(+)	Glabella & intracranial	6 × 4 4 × 4	–	Low atten.	15	–
2	12 mo	M	MR	Dermoid	Nasal mass	0 (closed)	7	(–)	Left lateral nasal bridge	10 × 10	Short, T1, T2	–	18	–
3	2 yr	F	CT and MR	DS epidermoid	Nasal mass	3	4	(–)	Glabella	3 × 4	Long T1, T2	Low atten.	22	–
4	2 yr	F	CT and MR	DS	Nasal dimple	2	4	(–)	–	–	–	–	18	–
5	3 yr	M	CT and MR	DS dermoid	Nasal dimple and mass	6	4	(–)	Glabella & nasal bridge	3 × 5	Short T1, T2	Low atten.	16	–
6	3 yr	M	MR	DS	Nasal dimple	0 (closed)	3	(–)	–	–	–	–	13	–
7	12 yr	F	CT and MR	DS	Nasal dimple	7	5	(–)	–	–	–	–	23	Colloid cyst
8	9 mo	F	CT	Nasal glioma	Nasal mass	Poorly defined	7	(–)	Left glabella	10 × 13	–	Soft-tissue Atten.	12	–
9	1 wk	F	CT and MR	NE	Nasal mass	15	Not seen	(–)	Glabella & ethmoids	30 × 50	Heterogeneous soft tissue & CSF	–	16	L temporal arachnoid cyst
10	6 wk	F	MR	NF	Nasal mass	5	2	(–)	Low frontal	20 × 20	Heterogeneous soft tissue & CSF	–	12	Subfrontal cyst
11	3 mo	F	CT and MR	NF and NE	Nasal mass	14	3	(–)	Glabella & ethmoids	20 × 35	Heterogeneous soft tissue	–	20	Bilateral temporal arachnoid cysts
12	4 mo	F	MR	NE	Meningitis, nasal mass	14	Not seen	–	Glabella & ethmoids	15 × 30	Heterogeneous soft tissue & CSF	–	28	ACC
13	6 mo	M	CT	NE	Nasal mass	20	3	(–)	Ethmoids & glabella	25 × 20	–	Heterogeneous soft tissue	20	ACC
14	6 mo	M	CT	NO	Proptosis, orbital masses	8	4	(–)	Bilateral orbits	10 × 15 mass each orbit	–	Heterogeneous mostly fluid	*	R. parietal schizencephaly
15	10 mo	F	MR	NF and NE	Nasal mass	15	3	(+)	Glabellar & low frontal	8 × 15	Mixed short & intermediate T1, T2	–	26	ACC, lipoma
16	24 yr	M	MR	NE	Nasal mass	20	Not seen	–	Glabellar	30 × 40	Heterogeneous soft tissue & CSF	–	25	–

Note.—FC = foramen cecum, DS = dermal sinus, NE = nasoethmoidal encephalocele, NF = nasofrontal encephalocele, NO = nasoorbital encephalocele, IOD = interorbital distance, ACC = agenesis of the corpus callosum.

* We were unable to measure IOD due to poorly defined medial orbital walls.

(Table 1). The eight patients (three males, five females) with encephaloceles all presented with nasal (six patients), low frontal (one), or orbital (one) masses. They ranged in age from 1 week to 24 years old at the time of their imaging study (mean, 3.5 years; median, 4 months). Four patients had MR scans only, two had CT scans only, and two had both MR and CT scans. The three patients (one male, two females) with nasal dermal sinuses presented with nasal dimples; the four patients (two males, two females) with associated dermoids presented with nasal masses. These seven patients ranged in age from 3 months to 12 years at the time of their imaging study (mean, 2.6 years; median, 3 years). Four patients had CT and MR, two had only MR, and one had only CT. The patient with the nasal glioma presented with a nasal mass and was 9 months old at the time of the study; she was studied only by CT.

Eleven of the 12 MR scans were obtained at 1.5 T using a 256 × 256 matrix. Axial 3-mm (1-mm gap) spin-echo (SE) 600/20/2 (TR/TE/excitations) MR images were obtained in all these patients. Axial SE 2500/20,70/2 images with a 3-mm slice thickness were obtained in two patients and a 5-mm slice thickness in nine patients. Sagittal SE 600/20 images with a 3- or 4-mm slice thickness were obtained in 10 patients (one did not have a sagittal imaging sequence) and coronal SE 600/20 images with a 4- or 5-mm slice thickness were obtained in 11 patients. A single patient (case 11) was scanned at 0.35 T. Axial SE 2000/40,80 and coronal SE 500/30 images were obtained by using a 7-mm slice thickness with a 3-mm gap and a 256 × 128 matrix.

CT scans were obtained in 10 patients. Among the eight patients with encephaloceles, four had CT. Of these, axial and coronal 5-mm contiguous images were obtained in three; the other was scanned using 1.5-mm contiguous images in the axial and coronal planes after intrathecal infusion of water-soluble contrast medium. The five patients with dermal sinus tracts and the one with the nasal glioma were scanned using 1.5-mm contiguous images in the axial and coronal planes. Sagittal reconstructions were performed in two patients. Two patients were scanned both before and after the intrathecal introduction of water-soluble contrast material. IV contrast administration was not used in any study.

CT scans of 29 patients (18 males, 11 females) and MR scans of 16 patients (nine males, seven females) without frontonasal disease were then reviewed to establish the normal appearance of the frontonasal structures in this age group (Table 2). The patients ranged from 1 to 25 months old at the time of their scan. These patients all presented with acquired orbital or intracranial disease unrelated to the nose or base of the anterior cranial fossa. The normal CT controls were assessed by axial images of 3-mm slice thickness; six patients had coronal 3- or 5-mm images as well. Both soft tissue and bone detail algorithms were present in all patients. The normal MR controls had sagittal 3-mm (13 patients) or 5-mm (three patients) SE 600/20 images. Axial 5-mm SE 2500–2800/20–30,60–100 images were available in all patients. Coronal 3-mm SE 600/20 images were available in seven patients. Axial 3-mm SE 600/20 images were available in five patients.

All scans were carefully scrutinized for normal landmarks, including the crista galli, nasal bones, frontal bones, nasal septum, foramen cecum, and glabella. The size of the foramen cecum was measured on axial scans as the distance from the most anterior aspect of the base of the crista galli to the most posterior aspect of the frontal bones. The greatest width and any abnormalities in the shape of the crista galli were recorded. The interorbital distance (defined as the narrowest distance between the medial walls of the orbits at the level of the cribiform plate) was measured. Any abnormal soft tissue or bony masses were noted.

Measurements of both the foramen cecum and the crista galli have a large potential for error because the value obtained may, theoretically, vary depending on the orientation of the imaging plane to the skull base. Fortunately, axial CT images at our institution are obtained routinely in a plane parallel to the canthomeatal line, resulting in a (usually) consistent orientation. Further possibility for error exists in the fact that the size of the foramen cecum and the width of the crista vary at different axial levels. Fortunately, the phenomenon of volume averaging results in visualization of the narrowest diameter of a foramen and the largest diameter of any bone structure within a slice; therefore, we feel that the measurements we have recorded are accurate and comparable. Indeed, upon scanning a skull phantom five times at slightly different scan angles, results varied by less than 20%. Moreover, all varied by less than 25% from the measurement obtained directly from the skull.

Results

Normal Patients

The normal nasofrontal region was found to have a complex but consistent structure on both CT and MR. The relevant structures include the cartilaginous nasal septum, the nasal bones, the external soft tissues of the nose, the nasal processes of the frontal bones, the cribriform plate, the foramen cecum, and the crista galli. In normal patients, the subcutaneous fat of the nose had sharp, discrete separation from the overlying skin anteriorly in all patients (Figs. 1 and 2). Posteriorly, the subcutaneous fat was bordered in the midline by the cartilaginous nasal septum and laterally by the cartilaginous bridges of the nose inferiorly and the nasal bones superiorly. The septum was of higher attenuation than fat on CT and of lower intensity than fat on short TR/TE and long TR/short TE MR images. The cartilage and fat were isointense on long TR/TE images. The nasal septum was always widened anteroinferiorly (Fig. 1). The paired nasal bones were always slightly separated at their most inferior margin (Figs. 1D and 2A).

In young patients, characteristic changes in signal intensity were often seen paracentrally (bilaterally and symmetrically) in the nasal processes of the frontal bone and, sometimes, in the nasal bones. These changes in signal intensity probably

TABLE 2: Summary of Control Patients

Imaging Method	No. of Patients	FC Size (mm)	Crista		
			Size (mm)	Bifid	IOD (mm)
CT	29	4 (SD = 3)	3 (SD = 2)	3/29	18 (SD = 4)
MR	16	3 (SD = 3)	3 (SD = 2)	0/16	19 (SD = 5)

Note.—FC = foramen cecum, IOD = interorbital distance.

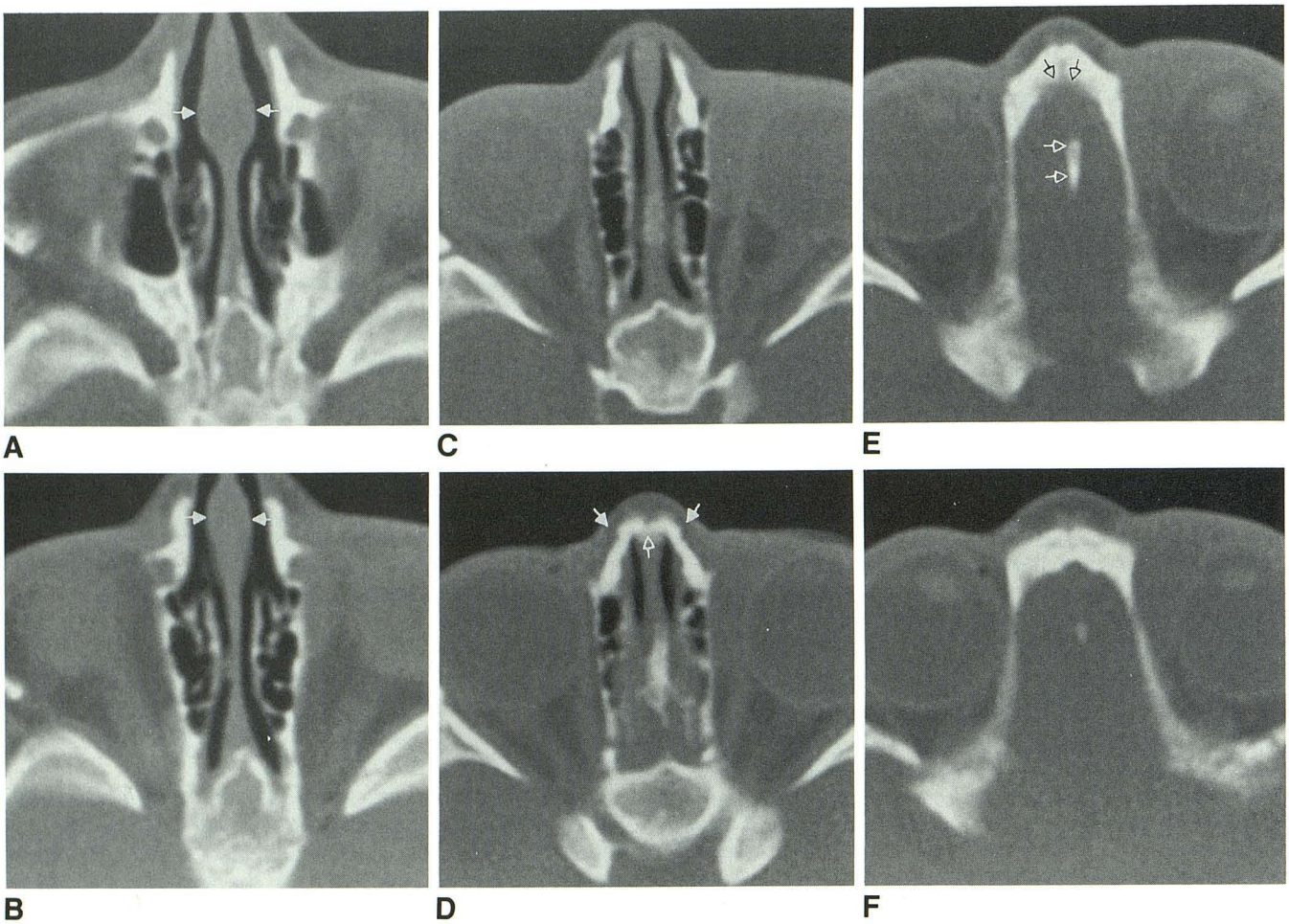

Fig. 1.—Thin section (3-mm) axial images through nose and base of anterior cranial fossa of a 4-month-old. The patient was scanned for orbital cellulitis.

***A* and *B*, The anteroinferior portion of the nasal septum is always focally widened (*arrows*) at all ages.**

***C* and *D*, A slight separation between the nasal bones is always present at their most anteroinferior margin (*open arrow*). This does not imply that a sinus tract is coursing through it. The subcutaneous fat under the skin of the nose (*closed arrows*) should be homogeneous and clearly separated from the skin at this age.**

***E* and *F*, These images are slightly superior to the foramen cecum. Crista galli is marked by *open white arrows*, and nasal processes of frontal bones by *open black arrows*. At this age there is very little diploic space within frontal bones or crista galli.**

represent fatty metamorphosis prior to pneumatization [7]. The pneumatizing bone marrow is of low attenuation compared with cortical bone on CT (Fig. 2) and has very short T1 and T2 relaxation times on MR (Figs. 3 and 4). The appearance on MR parallels that of the pneumatizing sphenoid bone [7].

The foramen cecum lies posterosuperior to the pneumatizing nasal processes of the frontal bone, being positioned between the frontal bone and the crista galli (Figs. 1–5). The size of the foramen ranged from 0 to 10 mm (average size, 4 mm; SD = 3 mm). It had the attenuation of fibrous tissue on CT (higher attenuation than brain) when large enough so that beam hardening from adjacent bone did not attenuate all the signal. On MR, the material in the foramen was always of low to medium intensity on all imaging sequences (Figs. 4 and 6), and was difficult to see on T1-weighted images before fatty changes occurred in the crista galli (Fig. 6).

The crista galli was located in the midline dorsal to the foramen cecum. It was bifid in three of the 29 patients imaged by CT. A bifid crista was never seen on MR. The side-to-side diameter of the crista (measured from the outer margin of the cortex on either side) varied from 1 to 8 mm (mean, 3 mm; SD = 2 mm). The signal of the marrow within the center of the crista was identical to that of the diploic space of the skull on CT (Figs. 2 and 5). It has a short T1 relaxation time (comparable to fat) on MR of all patients more than 14 months old (Figs. 3 and 4); it was isointense with brain in all patients 12 months old or younger. (No patients between 12 and 14 months old were scanned.) The signal of the crista on short TR images initially turned bright posteroinferiorly (Fig. 3); the high signal intensity then moved anteriorly and superiorly (Fig. 4).

The interorbital distance ranged from 12 to 26 mm (mean, 18 mm; SD = 4 mm).

Dermal Sinus Patients

All studies demonstrated soft-tissue intensity in the subcutaneous fat of the nose, representing the tract itself. In the

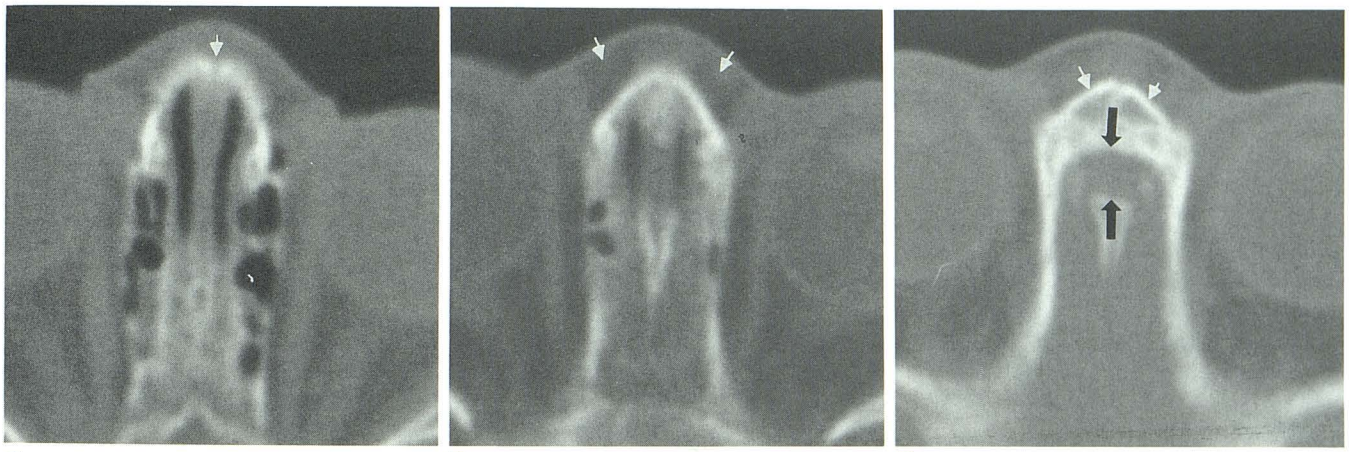

Fig. 2.—Axial CT scans through nose and cribriform plate region in an 11-month-old.
***A*, Note separation of inferior aspects of nasal bones (*arrow*), as seen in Fig. 1D. This is a consistent finding at all ages.**
***B*, By the age of 11 months, the marrow within the crista galli is more visible. The anterior cortical rim of the crista is often not visible at this level and does not imply erosion. Subcutaneous fat (*arrows*) is homogeneous.**
***C*, Low attenuation is seen in nasal processes of frontal bones (*white arrows*). This is a normal process that may represent the development of bone marrow or perhaps early pneumatization of bone. Foramen cecum is marked by *black arrows*.**

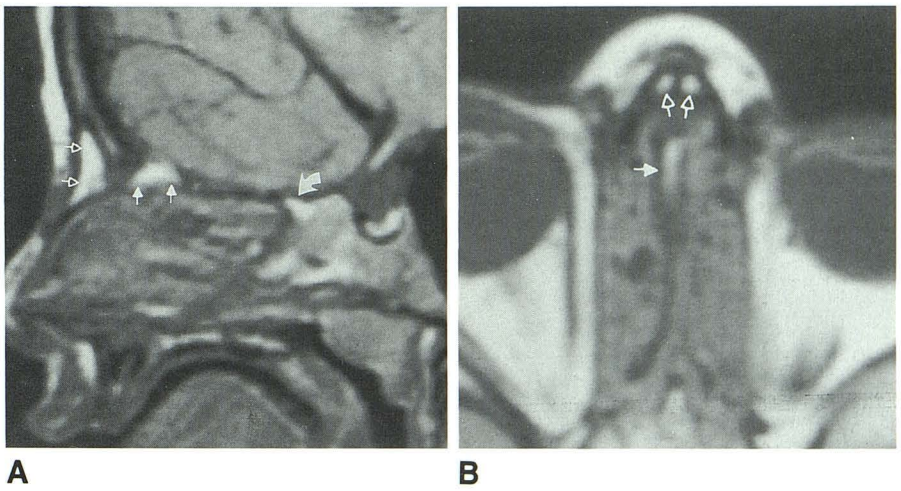

Fig. 3.—MR images through nasal region in a 12-month-old.
***A*, Sagittal T1-weighted image show high signal intensity in nasal processes of frontal bones (*open arrows*) and in posteroinferior crista galli (*closed arrows*). Note that high signal intensity is just beginning to develop in the anterosuperior sphenoid bone (*curved arrow*).**
***B*, The high signal intensity representing marrow and/or the process of penumatization is seen in the paired nasal bones (*open arrows*) and inferior crista galli/vertical plate of the ethmoid bone (*closed arrow*).**

four patients with associated dermoid (three) or epidermoid (one) tumors, the mass could be seen Figs. 7–9). The associated tumors were extracranial in three patients and both extra- and intracranial in one. The masses were all of low attenuation on CT with the exception of the extracranial component in patient 3 (Fig. 9), which was of soft-tissue density. The three dermoids exhibited short T1 and T2 relaxation times (Fig. 8) and the epidermoid had prolonged T1 and T2 relaxation times compared with brain (Fig. 7) on MR. The masses were all round to oval in shape and ranged from 3 to 10 mm in their largest diameter; the intracranial dermoid seemed to erode the adjacent inner table of the frontal bone (Fig. 9). The foramen cecum was patent in five of the seven patients, ranging in size from 2 to 7 mm (mean, 4 mm; SD = 2 mm) (Table 3). The diameter of the crista galli ranged from 3 to 7 mm (mean, 4 mm; SD = 2 mm); only the patient with the intracranial dermoid had a bifid crista. The interorbital distance ranged from 13 to 23 mm (mean, 18 mm; SD = 3 mm).

Nasal Glioma Patient

The single patient with a nasal glioma was studied only with CT. A 13-mm heterogeneous soft-tissue mass was seen extending continuously from the region of the foramen cecum inferiorly and anteriorly into the subcutaneous tissues at the glabella, just to the left of the midline. The mass appeared to extend intracranially on the coronal images (Fig. 10) and, indeed, a pedicle was seen to extend into an enlarged foramen cecum at surgery. The crista galli appeared truncated anteriorly where it bordered the nose (Fig. 10). The interorbital distance was 12 mm. The size of the foramen cecum could not be reliably determined in this patient because images were obtained in an oblique, half-axial plane.

Cephalocele Patients

Four cephaloceles extended inferiorly through the foramen cecum into the ethmoidal sinuses and beneath the nasal

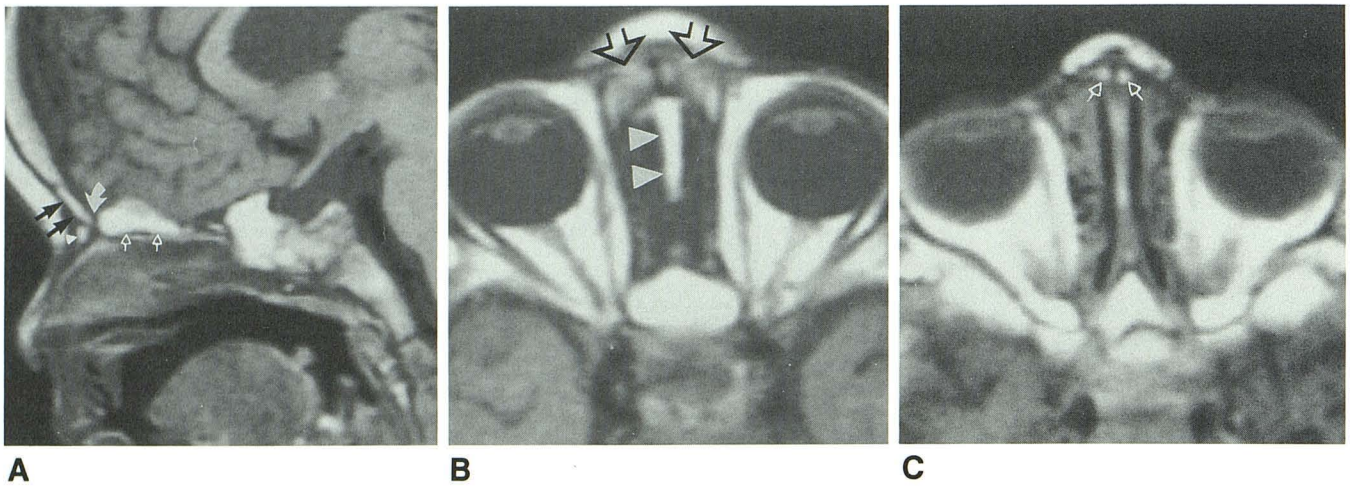

Fig. 4.—MR images through cribriform plate region in a 19-month-old child.

A, Sagittal SE 600/20 image shows high signal intensity in nasal processes of frontal bones (*black arrows*), nasal bones (*arrowhead*), and crista galli/vertical plate of the ethmoid bone (*open arrows*). Note that the high signal intensity in the crista galli has markedly increased as compared with the 11-month-old patient shown in Fig. 3. The foramen cecum is within the area of low signal intensity demarcated by the *curved arrow*. Incidentally noted is marked high signal intensity in the presphenoid bone, which will soon begin to undergo cavitation.

B, Axial SE 600/20 image shows patchy high signal intensity in nasal processes of frontal bones (*black arrows*) and marked high signal intensity in inferior crista galli/vertical plate of the ethmoid (*white arrowheads*).

C, Axial SE 600/20 image, slightly inferior to (*B*). Paired areas of hyperintensity (*arrows*) represent marrow that is probably cavitating in the nasal bones.

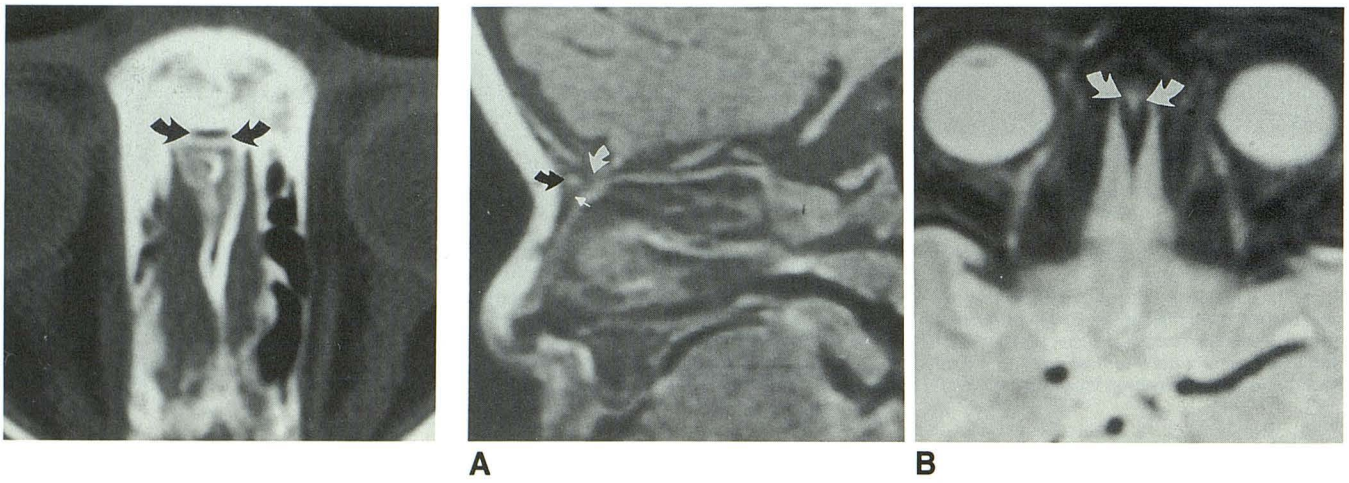

Fig. 5.—CT scan of a small foramen cecum in a 2-year-old. The foramen is seen as an oblong lucency (*arrows*) immediately anterior to inferior aspect of crista galli. This was among the smallest foramina seen in our series.

Fig. 6.—MR images of crista galli/foramen cecum area in a 7-month-old patient.

A, Before fat is deposited in the frontal bones, nasal bones, and crista galli, the foramen cecum is difficult to see. On this sagittal SE 600/20 image, the nasal process of the frontal bone is marked by the *curved black arrow*, the nasal bone is marked by the *straight white arrow*, and the probable location of the foramen cecum is shown by the *curved white arrow*.

B, At this age, the location of the foramen cecum is identified better on T2-weighted images. Here the foramen (*arrows*) is demarcated by the crista galli posteriorly and the nasal processes of the frontal bones anteriorly. Because both bony structures are very dark on this T2-weighted image, the foramen is more easily seen.

bones into the nasal soft tissues (Fig. 11); these were labeled as nasoethmoidal encephaloceles [8]. One cephalocele extended anteriorly between the frontal bones and above the nasal bones into the soft tissues in the glabellar and inferior frontal region and was labeled a nasofrontal encephalocele (Fig. 12). Two lesions extended both inferiorly through the foramen cecum beneath the nasal bones and anteriorly between the frontal and nasal bones; we considered these to be both nasofrontal and nasoethmoidal encephaloceles (Fig. 13). The final lesion, a nasoorbital encephalocele, extended through the foramen cecum, then inferiorly and laterally behind the frontal processes of the maxillary bones into both orbits, laterally displacing the globes (Fig. 14). All of the extracranial masses were lobulated and had a mixed signal intensity of both soft tissue and water intensities. Fat from an interhemispheric lipoma extended into the cephalocele in patient 15 (Fig. 13). The extracranial masses ranged in size from 8×15 mm to 30×50 mm.

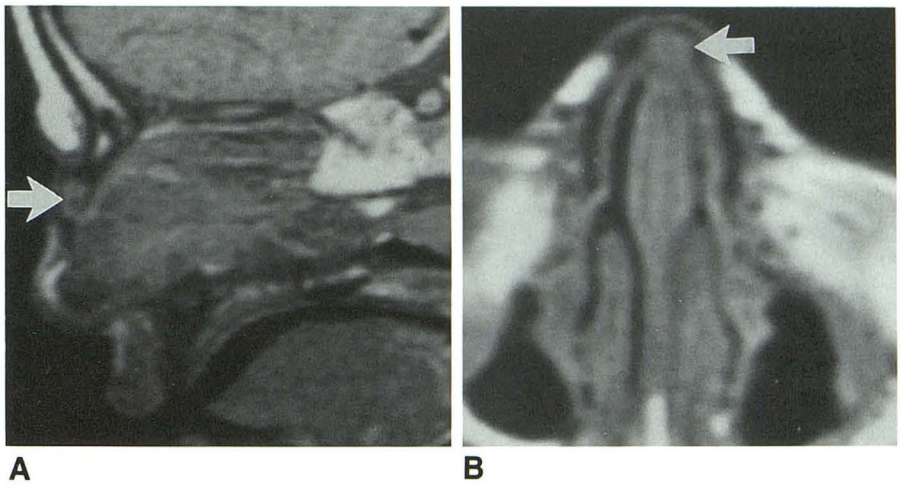

Fig. 7.—Patient 3: 2-year-old girl with dermal sinus and epidermoid.

***A*, Sagittal SE 600/20 image shows a small mass, isointense with nasal cartilage and hypointense compared with brain, adjacent to nasal cartilage in the midline anteriorly (*arrow*). The associated dermal sinus is not visualized. The sinus tracts themselves were not seen on either MR or CT scans in any patient.**

***B*, Axial SE 600/20 image shows epidermoid tumor, which actually lies within the nasal cartilage in the midline (*arrow*) immediately inferior to the nasal bones.**

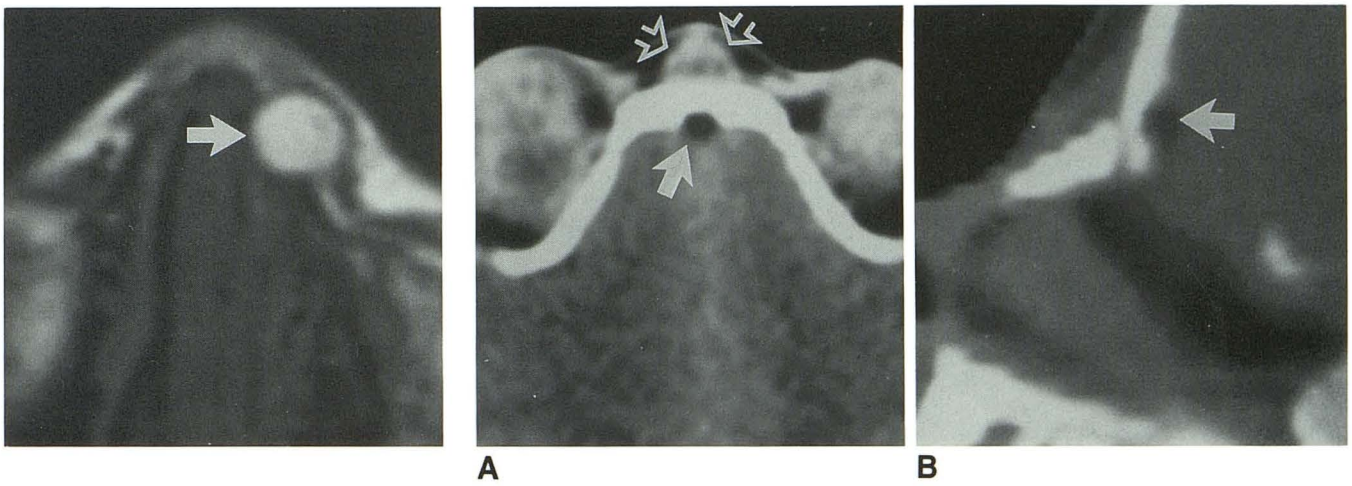

Fig. 8.—Patient 2: 12-month-old boy with nasal dermoid. Axial SE 600/20 image shows a round mass (*arrow*) with short T1 relaxation time sitting within left lateral nasal cartilage. T2-weighted images (not shown) showed a short T2 relaxation time. At surgery, this was found to be a dermoid.

Fig. 9.—Patient 1: 3-month-old girl with dermal sinus and intra- and extracranial dermoid.

***A*, Axial image from a CT scan performed with intrathecal iohexol because an encephalocele was initially suspected. A small, round hypodense mass (*closed arrow*) is seen in the midline immediately above the foramen cecum. The adjacent frontal bones are smoothly eroded. An associated soft-tissue mass is seen in adjacent extracranial soft tissues (*open arrows*).**

***B*, Sagittal reformation using bone windows shows mass (*arrow*) sitting in anteroinferior portion of anterior cranial fossa, immediately above the foramen cecum. Identification of intracranial dermoids is important because it suggests the appropriate surgical management of these patients.**

TABLE 3: Summary of Patients with Nasal Masses

Diagnosis	No. of Patients	FC Size (mm)	Crista		
			Size (mm)	Bifid	IOD (mm)
Cephalocele	8	12 (SD = 5)	3 (SD = 2)	1/8	21 (SD = 7)
Dermal sinus	7	3 (SD = 2)	4 (SD = 2)	1/7	18 (SD = 3)
Nasal glioma	1	Not measurable	4	1/1	12

Note.—FC = foramen cecum, IOD = interorbital distance.

The foramen cecum was enlarged in all patients with nasoethmoidal encephaloceles and in the patient with the nasoorbital encephalocele, ranging from 8 to 20 mm in diameter (mean, 12 mm; SD = 5 mm). The crista galli was either absent (possibly eroded) or present but small in all patients in this group. In all of the patients with a detectable crista galli, the anterior margin of the crista was smoothly concave, suggesting erosion of bone by the cephalocele (Fig. 14). In patient 15, the remaining crista appeared bifid. The interorbital distance ranged from 12 to 28 mm (mean, 21 mm; SD = 7 mm).

A high rate of associated brain anomalies was present in this group. Three patients with nasoethmoidal encephaloceles had agenesis of the corpus callosum; one of these (patient 15) had an interhemispheric lipoma (Fig. 13) and carried a

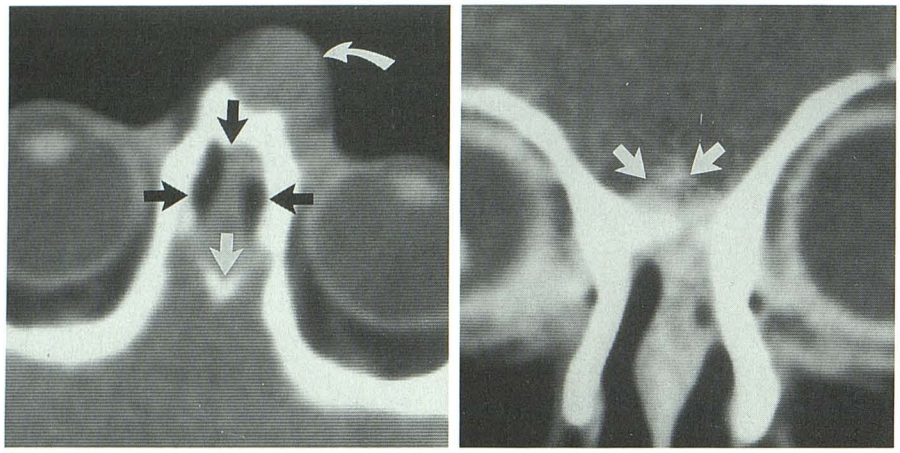

Fig. 10.—Patient 8: 9-month-old girl with nasal glioma.

A, Axial CT scan shows a markedly widened foramen cecum (*black arrows*) with an extremely small (possibly eroded) crista galli (*straight white arrow*). *Curved white arrow* points to the mass in the glabellar region.

B, Coronal CT image shows apparent extension of the mass (*arrows*) intracranially through the foramen cecum. On CT, this mass could not be differentiated from an encephalocele.

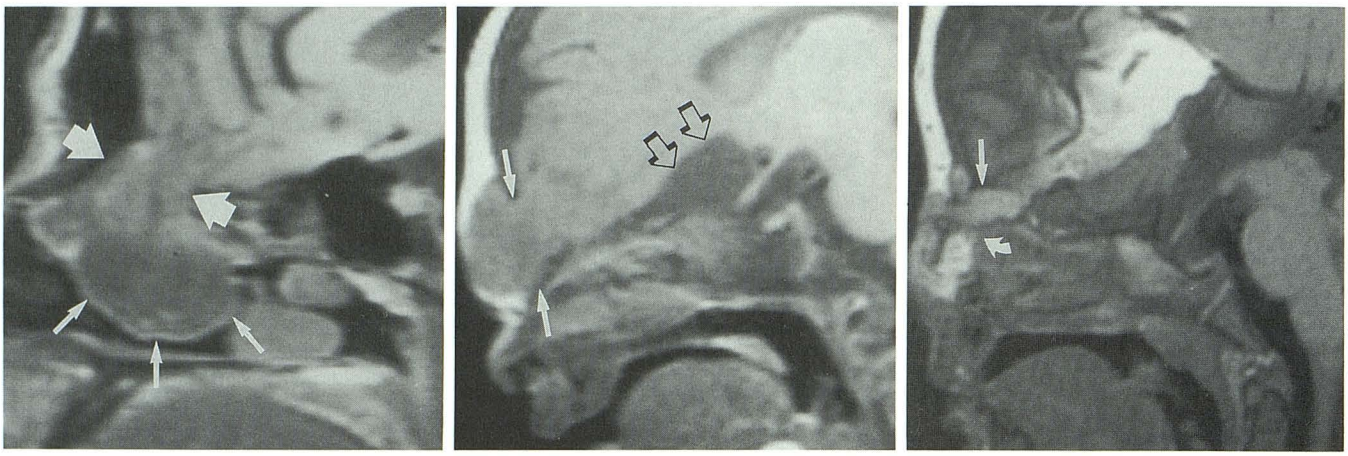

Fig. 11.—Patient 16: 24-year-old man with nasoethmoidal encephalocele. Sagittal SE 600/20 MR image shows that the foramen cecum is markedly widened (*wide arrows*). A heterogeneous mass is seen to extend inferiorly through the foramen cecum into the nasal cavity and ethmoid air cells (*thin arrows*). The brain is stretched as it enters the mass. The nasoethmoidal encephaloceles all seemed to widen the foramen cecum.

Fig. 12.—Patient 10: 6-week-old girl with nasofrontal encephalocele. A soft-tissue mass that is continuous with brain is seen extending anteriorly between the frontal bones into the soft tissues in the subfrontal and glabellar regions. The disruption of the calvaria (*white arrows*) is at the site where the fonticulus frontalis was located and may be a persistence of that primitive fontanelle. A subfrontal cyst (*open black arrows*) is present beneath the gyrus rectus.

Fig. 13.—Patient 15: 10-month-old girl with nasofrontal and nasoethmoidal encephaloceles and midline craniofacial dysraphism. Sagittal SE 600/20 MR image shows absence of corpus callosum. A large interhemispheric lipoma is seen in the frontal region. The lipoma extends out of the calvaria in the interfrontal region at the location of the fonticulus frontalis (*straight arrow*) and inferiorly into the nasal region near the site of the foramen cecum (*curved arrow*). (Reprinted with permission from [26].)

clinical diagnosis of median cleft face syndrome. Two patients had large middle temporal fossa arachnoid cysts, one unilaterally and one bilaterally. One patient had a subfrontal cyst (Fig. 12). Finally, one patient had a unilateral right parietal schizencephaly.

Discussion

Embryology of the Nasofrontal Region

The membranous neurocranium (the cranial vault) originates as a capsular membrane around the developing brain. In the very early stages of gestation it is composed of two tissue layers, which are of both mesodermal and ectodermal origin. At the sixth or seventh gestational week, the external layer differentiates into an inner membrane of primitive dura and an outer membrane with osteogenic properties. The nasal and frontal bones will develop from intramembranous ossification of the latter during the seventh or eighth week of gestation [3, 9, 10].

Posterior to the nasal and frontal bones lies the anterior wall of the nasal capsule (Fig. 15). This capsule is a part of the chondrocranium (skull base), which forms the floor of the developing brain. During the eighth gestational week, the nasal capsule may be considered a box of cartilage divided by a median cartilaginous septum. As the lateral walls of the capsule ossify later in development to form the lateral masses of the ethmoid and the inferior concha bones, the anterior two-thirds of the midline nasal septum will remain cartilaginous. The posterior portion of the septum, formed by the fusion of the presphenoid cartilages in the midline, will ossify

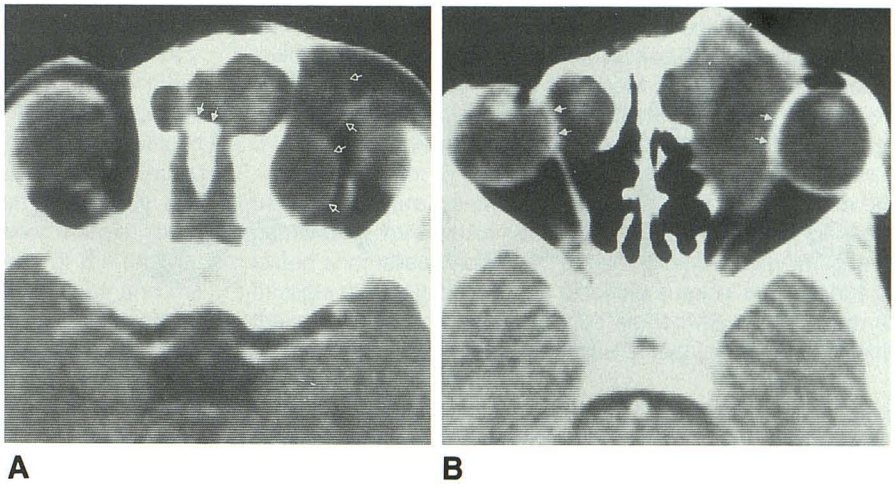

Fig. 14.—Patient 14: 6-month-old boy with nasoorbital encephalocele.

***A*, Axial contrast-enhanced CT scan through level of foramen cecum shows erosion of the anterior aspect of the crista galli (*closed arrows*). Soft tissue is seen extending through foramen cecum on the left toward the orbit. Water-density masses are seen within the left orbit (*open arrows*), displacing the globe laterally.**

***B*, At a slightly lower level, heterogeneous masses composed of CSF and dysplastic brain tissue are seen in the medial aspects of the orbits, displacing the globes (*arrows*) bilaterally.**

at birth to become the perpendicular plate of the ethmoid bone. Its upper edge will form the crista galli [3, 9, 11].

Two transient spaces are formed by the developing structures in the nasofrontal region (Fig. 15). The first is a small fontanelle, the fonticulus nasofrontalis, which lies in the midline between the paired frontal and nasal bones [3, 9, 12–14]. The second is the prenasal space, bounded posteriorly by the anterior wall of the nasal capsule and anteriorly by the nasal bones and fonticulus [1–3, 12, 15].

Toward the end of the second gestational month, a diverticulum of dura extends anteroinferiorly through the prenasal space and transiently contacts the superficial ectoderm in the region that will become the nose. As normal development progresses, the nasal processes of the frontal bone grow inferiorly to surround the dural projection and form a canal, the foramen cecum [1–3, 15]. The dural projection eventually involutes into a fibrous structure that fills the obliterated foramen. In normal children, the bony foramen is, therefore, filled by fibrous tissue [1, 3].

Nasal dermoids, nasal encephaloceles, and nasal gliomas result from aberrations of this normal development process [2, 3]. The most widely accepted theory at present is that proposed by Brunner and Harned [16] and elaborated upon by Pratt [1] and Sessions [3]. These authors suggest that nasal dermal sinuses and some nasal gliomas and encephaloceles result from incomplete regression of the projection of dura that transiently traverses the prenasal space. If the dural projection remains adherent to the skin, a small dimple will be present on the external surface of the nose; this dimple is the external orifice of a dermal sinus tract (Fig. 16). The tract can terminate anywhere along the path of the dural projection or can extend upward, through the foramen cecum, into the cranial vault. Dermoid and epidermoid tumors result from desquamation of cells of the dermis and epidermis lining the tract. They may develop anywhere along the tract. If large, the associated dermoid may occasionally extend posteriorly, beneath the crista galli, or anteriorly, through the fonticulus.

Nasal cephaloceles and gliomas are also explained by this concept. Cephaloceles presumably result from herniation of intracranial tissues into the dural projection through the fora-

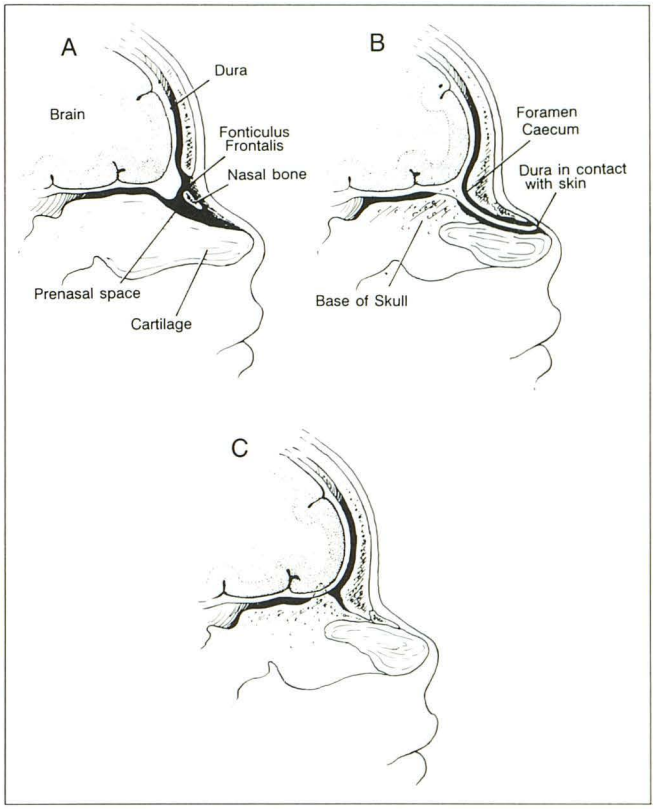

Fig. 15.—Schematics showing normal development of the base of the skull and prenasal space. (Adpated from [2].)

***A*, A small fontanelle, the fonticulus frontalis, is transiently present between the developing frontal bones and the developing nasal bones. A second transient space, the prenasal space, is present at the same time, lying between the developing nasal bones and the cartilage of the developing nasal capsule.**

***B*, Slightly later in development, the fonticulus frontalis has closed. The prenasal space has narrowed as a result of growth of the nasal processes of the frontal bones. This space, now completely surrounded by bone, is termed the foramen cecum. A projection of dura extends from the intracranial space through the foramen cecum and comes in contact with the skin in the region that will form the nose.**

***C*, Slightly later in development, the dural projection separates from the skin of the nose and retracts back into the cranium. After this retraction and involution of the dural projection, the foramen cecum partially fuses and the prenasal space is obliterated.**

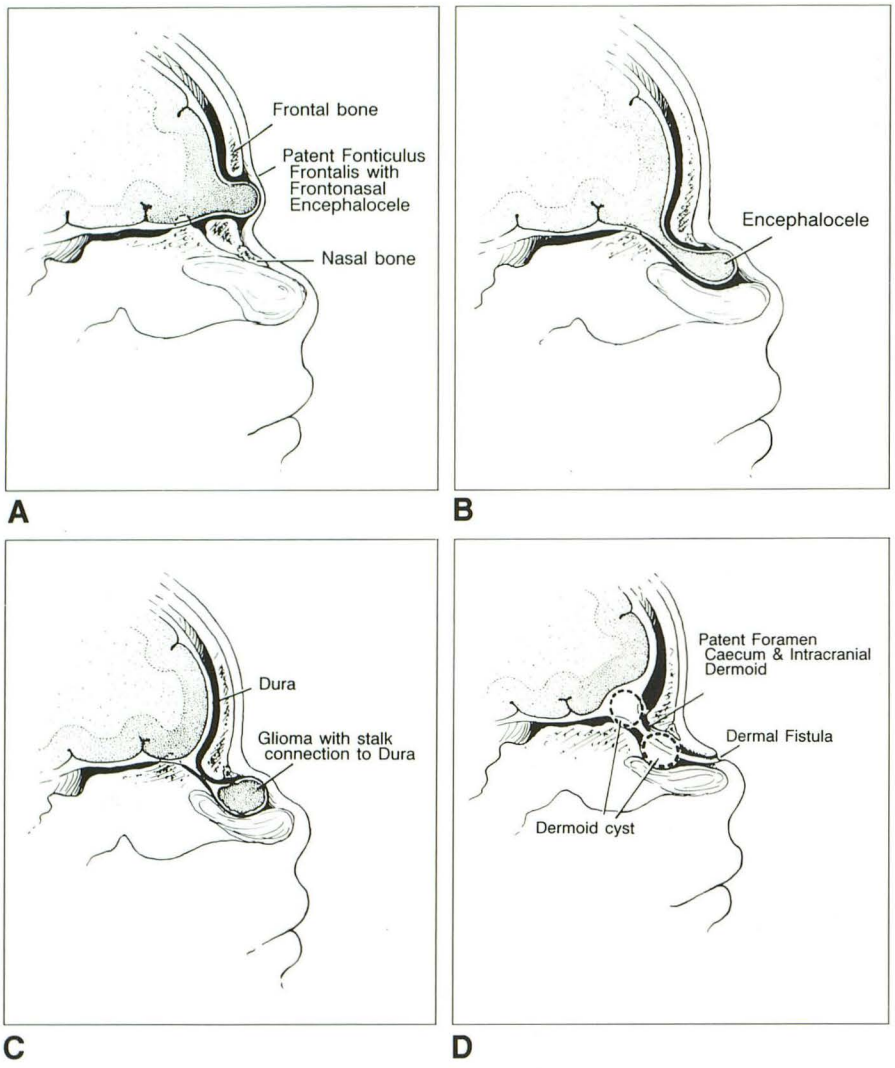

Fig. 16.—Schematics illustrating the results of aberrant development in the anterior skull base.

***A*, If the fonticulus frontalis fails to close, the result is a frontonasal encephalocele.**

***B*, A failure of the foramen cecum to close results in a frontoethmoidal encephalocele.**

***C*, If the dural projection through the foramen cecum involutes late in development or only involutes proximally, the result is a nasal glioma with a fibrous stalk connecting it to the intracranial contents across the foramen cecum.**

***D*, Dermal sinuses result from a lack of involution of the dural projection through the foramen cecum. Any part of the dermal sinus may involute. A dermoid or epidermoid tumor may form anywhere along the tract of the dermal sinus as a result of desquamation of the lining of the tube.**

men cecum (nasoethmoidal and nasoorbital cephaloceles) or hernation through the fonticulus (nasofrontal cephalocele) (Fig. 16). Although nasoethmoidal cephaloceles can be explained by a mere lack of regression of the most cranial aspect of the dural projection, the explanation of nasofrontal and nasoorbital cephaloceles requires either an abnormal development of the respective fontanelles or orbital structures or an increase in intracranial pressure resulting in the focal brain herniation.

Nasal gliomas (also known as nasal cerebral heterotopias) are composed of dysplastic brain tissue within the nasal cavity or subcutaneous tissue over the glabellar region, separate from intracranial contents. In about 15% of patients with nasal gliomas, a connection with intracranial structures persists in the region of the foramen cecum [17]. Sessions [3] suggests that these lesions probably result from herniation of the brain through the foramen cecum into the dural projection with subsequent regression (in most patients) of the more craniad portion of the projection. The result is a sequestration of the glial tissue within the nose or nasal soft tissues.

Present Data

Congenital midline nasal masses are rare but important anomalies that almost always present in childhood. Patients with nasal encephaloceles and nasal gliomas typically present with nasal (rarely orbital) masses. Patients with dermal sinuses most commonly present because of nasal dimples or masses; occasionally, however, the dermal sinuses and cephaloceles become infected and this infection is the reason for presentation. The infection is usually superficial (localized to the skin or sinus ostia); rarely, the infection extends intracranially [2, 3, 12].

Radiologic evaluation is important in the work-up of midline nasal masses. Classically, plain films were obtained to look for widening of the nasal septum, erosion or separation of contiguous bones, increased interorbital distance, or a bony defect in the cribiform plate [18]. The facial bony defects are useful in the classification of frontoethmoidal cephaloceles into three subtypes [19]. In the nasofrontal group, the defect lies between the frontal and nasal bones with the frontal

bones being displaced superiorly and the nasal bones and nasal cartilage displaced inferiorly. Nasoethmoidal cephaloceles course through a defect that lies between the nasal bones and the nasal cartilage. The nasal and frontal bones (and the frontal processes of the maxillae) are displaced superiorly and anteriorly, whereas the nasal cartilage, nasal septum, and ethmoid bones are displaced posteriorly and inferiorly. In the nasoorbital form, the anterior margin of the bony defect is formed by the frontal process of the maxilla; the posterior margin is formed by the lacrimal bone and the lamina papyracea of the ethmoid bone. Therefore, the location of a bony defect as determined by plain radiographs is valuable both in the detection of frontoethmoidal cephaloceles and in the determination of their subtype. CT and MR scans may show any intra- or extracranial soft-tissue masses, defects in or separation of bones, enlargement of the foramen cecum, or distortion of the crista galli [2, 12].

In the present series, both MR and CT were able to clearly differentiate dermoids and dermal sinuses from the cephaloceles. The cephaloceles had marked widening of the calvarial openings (foramen cecum or fonticulus frontalis) through which the brain herniation occurred. The crista galli was always eroded, the interorbital distance was mildly increased, and a soft-tissue mass was seen to extend into the nasal cavity, nasal or frontal soft tissues, or orbits (Figs. 11–14). It is unfortunate that an accurate measurement of the size of the foramen cecum was not available in the patient with the nasal glioma. We suspect that it would have been enlarged, because the anterior portion of the crista galli was eroded and a stalk was seen to extend upward through the foramen at surgery. However, because 85% of nasal gliomas do not connect with intracranial structures [17], it is unlikely that foramen cecum size is ever useful in differentiating nasal gliomas from dermoids or cephaloceles.

The location of the cephalocele as determined by MR scans seems to verify the theories of Brunner and Harned [16], Pratt [1], and Sessions [3] regarding pathogenesis. All the nasoethmoidal cephaloceles clearly extended into the nasal cavity via the foramen cecum. All the nasofrontal cephaloceles coursed through the site of the fonticulus frontalis. In two patients, the intracranial tissue coursed through both spaces simultaneously. In the nasoorbital cephalocele, brain tissue presumably initially traversed the foramen cecum before deviating laterally into the orbits.

Another interesting feature of these cephaloceles was the high rate of associated brain anomalies. Three patients had large intracranial cysts, two had agenesis of the corpus callosum, one had agenesis of the corpus callosum with an interhemispheric lipoma, and one had right parietal schizencephaly. Both the callosal agenesis and the schizencephaly have been associated with teratogenic effects during the late second gestational month [20, 21], the same time at which the prenasal space and fonticulus frontalis form. This temporal relationship suggests that these associations should be common, and, indeed, a high frequency of agenesis of the corpus callosum in patients with basal encephaloceles has been reported [22]. The high rate of associated brain anomalies observed in this series is in disagreement with some earlier reports [19, 23], which describe a frequent, but significantly lower rate. Previous reports stressed hydrocephalus and ocular anomalies as being the most common. We suspect that the present study is more accurate because of the use of more sensitive modern imaging techniques.

MR is superior to CT in the evaluation of nasal cephaloceles because it more clearly and noninvasively demonstrates the pathway of intracranial herniation and the presence of associated anomalies. Moreover, obtaining high-quality images in multiple planes is valuable in planning surgical approaches to these lesions. For these reasons alone, MR would seem to be the technique of choice for initial screening of patients with midline nasal masses.

With CT, it was only possible to differentiate the nasal glioma from an encephalocele after infusion of intrathecal contrast material; encephaloceles fill with contrast whereas nasal gliomas do not. Although part of the difficulty in the present series may have been caused by poor angling of the CT gantry, a difficulty in differentiation should be expected because, embryologically, nasal gliomas are encephaloceles in which the connection to the brain has partially or completely sealed off. Therefore, the foramen cecum may remain enlarged and the crista galli may be eroded in the presence of a large soft-tissue mass in the nasal cavity. The lack of communication with the subarachnoid space (ruling out a cephalocele) can be demonstrated only by the absence of flow of contrast material into the nasal mass. We suspect that it will be difficult to demonstrate the presence or lack of this communication by MR.

Nasal dermal sinuses and nasal dermoids turned out to be very difficult to evaluate both by CT and MR. The most important information to be obtained in these studies (in fact the major reason the studies are requested) is to assess the extent of the dermal sinus or dermoid and, in particular, to determine whether intracranial extension of the sinus or intracranial tumor is present. In the absence of intracranial disease, the surgical therapy consists of exposing and removing the sinus tract as it courses upward to the skull base. If the tract extends upward through the foramen cecum but there is no intracranial tumor, many surgeons will merely tie off the tract at the skull base [12]. If there is intracranial tumor, however, a combined intracranial-extracranial approach is mandatory in order to adequately treat the patient. Therefore, it is very important to assess the full extent of dermoid or epidermoid tumor but less important to determine whether the sinus tract extends intracranially.

Examination of our data reveals that the classically used criteria of foramen cecum size, abnormality of the shape or bifidity of the crista galli, and interorbital distance were identical in our control group and dermal sinus group. Therefore, we must concur with Pensler et al. [12] that these findings are helpful only when positive. We add, furthermore, that these findings are rarely present.

Both CT and MR were excellent in the detection of dermoid and epidermoid tumors in the nose. The single dermoid that extended intracranially was well visualized by CT in spite of its small (4×4 mm) size. Thus, our results substantiate those of others [12, 24] who have found CT to be accurate in the

detection of intracranial tumors in patients with dermal sinus tracts. We expect that MR should be as sensitive as or more sensitive than CT in the detection of these masses.

It is important to note that neither CT nor MR accurately delineated the dermal sinus itself as it coursed through the nose or foramen cecum. Moreover, both imaging methods (particularly MR) were replete with potential pitfalls, most of which were related to the fatty metamorphosis of the marrow [25] and the signal intensity changes accompanying aeration of the frontal sinuses [7]. Unfortunately, these changes occur from approximately 12 months to 5 years of age, the same ages at which most patients with dermal sinuses present [5, 12, 24].

One potential pitfall is the shape of the nasal septum. In normal patients, the nasal septum widens in its inferior portion 5 to 10 mm posterior to the junction with the bridge of the nose (Fig. 1). This normal widening should not be mistaken for expansion resulting from inclusion of a sinus tract within the septum.

A second potential pitfall results from the low density (on CT) and diminution of T1 and T2 relaxation times (on MR) associated with fatty change in the inferior frontal sinuses and, sometimes, nasal bones prior to pneumatization (Figs. 2–4). The best way to differentiate these areas from fatty tumors is to recognize the characteristic location; dermoids will usually pass posterior to these pneumatizing spaces. Furthermore, the pneumatizing spaces are usually paired with a small bony septum between them (Figs. 2–4); such septa are never seen in dermoids.

The final major potential pitfall, which is the most serious because it may result in an unncessary craniotomy, is mistaking the crista galli or subjacent perpendicular plate of the ethmoid bone for a dermoid. The central portion of these bones begins to undergo fatty change at approximately the 12th postnatal month. The fatty change appears initially in the posterior and inferior portion of the perpendicular plate and seems to progress anteriorly and superiorly until fatty signal is seen throughout. It is easy, particularly on coronal MR, to mistake this high signal intensity for a dermoid with intracranial extension because of the proximity to the foramen cecum. It is critical to locate the foramen and crista in the sagittal and axial planes in order to ascertain whether the high signal truly represents a dermoid as opposed to marrow within bone. If necessary, a high-resolution CT scan with thin sections should be obtained to verify whether intracranial tumor is present.

In conclusion, we have reviewed imaging studies performed on 16 patients with congenital midline nasal masses and 45 normal patients. CT and MR seem equally sensitive in the detection of these masses. MR was superior in delineating the extent and morphology of encephaloceles; moreover, a high rate of occurrence of associated anomalies, which are more easily detected by MR, were present in patients with encephaloceles. CT and MR were equally sensitive in the detection of dermoid and epidermoid tumors associated with dermal sinus tracts; however, neither technique was able to resolve the sinus tracts themselves. Care should be taken not to mistake pneumatizing bone or fatty bone marrow for dermoid tumors in these patients.

REFERENCES

1. Pratt LW. Midline cysts of the nasal dorsum: embryologic origin and treatment. *Laryngoscope* **1965**;75:968–980
2. Hughes GB, Sharpino G, Hunt W, Tucker HM. Management of the congenital midline nasal mass: a review. *Head Neck Surg* **1980**;2:222–233
3. Sessions RB. Nasal dermal sinuses: new concepts and explanations. *Laryngoscope* **1982**;92(Suppl 29):7–28
4. Bradley PJ. Results of surgery for nasal dermoids in children. *J Laryngol Otol* **1982**;96:627–633
5. Bradley PJ, Singh SD. Congenital nasal masses: diagnosis and management. *Clin Otolaryngol* **1982**;7:87–97
6. Bradley PJ. The complex nasal dermoid. *Head Neck Surg* **1983**;5:469–473
7. Aoki S, Dillon WP, Barkovich AJ, Norman D. Marrow conversion before pneumatization of the sphenoid sinus: assessment with MR imaging. *Radiology* **1989**;172:373–375
8. Diebler C, Dulac O. Cephaloceles: clinical and neuroradiological appearance. *Neuroradiology* **1983**;25:199–216
9. Sperber GH. *Craniofacial embryology*, 3rd ed. Bristol: Wright PSG, **1981**
10. Gasser RF. Early formation of the basicranium in man. In: Bosma JF, ed. *Symposium on development of the basicranium*. Bethesda: U.S. Department of Health, Education and Welfare, **1976**
11. Pansky B. *Review of medical embryology*. New York: McMillan, **1982**
12. Pensler JM, Bauer BS, Naidich TP. Craniofacial dermoids. *Plast Reconstr Surg* **1988**;82(6):953–958
13. Bosma JF. Introduction to the symposium on development of the basicranium. In: Bosma JF, ed. *Symposium on development of the basicranium*. Bethesda: U.S. Department of Health, Education and Welfare, **1976**
14. Bosma JF. Anatomy of the infant head. Baltimore: The Johns Hopkins University Press, **1986**
15. Littlewood AH. Congenital nasal dermoid cysts and fistulas. *Plast Reconstr Surg* **1961**;27:471–488
16. Brunner H, Harned JW. Dermoid cysts of the dorsum of the nose. *Arch Otolaryngol* **1942**;36:86–93
17. Gorenstein A, Kern EB, Facer GW, Lows ER Jr. Nasal gliomas. *Arch Otolaryngol* **1980**;106:536
18. Johnson GF, Weisman PA. Radiological features of dermoid cysts of the nose. *Radiology* **1964**;82:1016–1021
19. Suwanwela C, Suwanwela N. A morphological classification of sincipital encephalomengoceles. *J Neurosurg* **1972**;36:201–211
20. Barkovich AJ, Norman D. MR of schizencephaly. *AJNR* **1988**;9:297–302
21. Barkovich AJ, Norman D. Anomalies of the corpus callosum: correlation with further anomalies of the brain. *AJNR* **1988**;9:493–501
22. Yokota A, Matsukodo Y, Fuwa I, Moroki K, Nagahiro S. Anterior basal encephalocele of the neonatal and infant period. *Neurosurgery* **1986**;19:468–478
23. Rapport RL, Dunn RC Jr, Alhady F. Anterior encephalocele. *J Neurosurg* **1981**;54:213–219
24. McQuown SA, Smith JD, Gallo AE. Intracranial extension of nasal dermoids. *Neurosurgery* **1983**;12:531–535
25. Okada Y, Aoki S, Barkovich AJ, et al. Cranial bone marrow in children: assessment of normal development with MR imaging. *Radiology* **1989**;171:161–164
26. Barkovich AJ. *Pediatric neuroimaging*. New York: Raven Press, **1990**:88